Density functional study of the nitrosamine–formic acid and nitrosamine–formamide interactions

Sadeghali Bavafa [a,*], Reza Behjatmanesh-Ardakani [b], Farzane F. Mashhadi [c]

[a] International University of Chabahar (IUC), Chabahar, Iran
[b] Department of Chemistry, School of Science, Payame Noor University (PNU), Ardakan, Yazd, Iran
[c] Department of Pharmacology, University of Medical Sciences, Zahedan, Iran

ARTICLE INFO

ABSTRACT

During the computation, 15 complexes for nitrosamine–formic acid (Z, E), and nitrosamine–formamide were found. For all of the methods, containing B3LYP/6-311++(2d,2p), B3LYP/aug-cc-pVDZ and B3LYP/aug-cc-pVTZ, the complexes of Z-1 and F-1 are the most stable ones. The order of hydrogen bond strengths are as follows: O–H···O > N–H···O > N–H···N > C–H···O > C–H···N. Results show that the proton stretching between a donor and an acceptor affects the strength of hydrogen bond. In some cases, eight-member ring is formed due to the resonance-assisted hydrogen bonds (RAHB) mechanism. AIM analyses at the hydrogen bond critical points show maximum electron density (ρ) for O–H···O, and minimum electron density for C–H···O.

1. Introduction

A hydrogen bond is weaker than a common chemical bond, and can be formed in solids, liquids, and gas phases. It is commonly represented as X–H···Y, where X and Y are atoms having electronegativity higher than that of hydrogen (e.g., O, N, F, Cl, S). The X–H group is termed "electron acceptor" or "hydrogen bond donor", while Y is the "electron donor" or "hydrogen bond acceptor". The electronegative X atom attracts electrons from the hydrogen, by which gains partial positive charge and, in turn, it attracts a lone pair of electrons from the Y atom. Formic acid (systematically called methanoic acid) is the simplest carboxylic acid. Its formula is HCOOH or CH_2O_2. Formic acid is the simplest organic acid exhibiting rotational isomerism by rotating around the single C–O bond. It is a molecule of astrophysical [1] and atmospheric [2] relevance, and has a wide range of industrial applications. Formic acid exists in two stable planar structures, the *cis* (E-rotamer) and *trans* (Z-rotamer) conformers, with 0° and 180° H–C–O–H dihedral angles, respectively. The *trans* form is more stable and it is the predominant one in the gas phase [3]. At a glance, one may suggest that the Z-rotamer complex is more stable than the E-rotamer, however, this needs exact calculation with different theoretical approaches such as NBO, and AIM to calculate how much it is more stable. This work tries to answer this question.

Formamide, also known as methanamide, is an amide derived from formic acid. Its formula is $HCONH_2$ or CH_3NO. It is a clear liquid which is miscible with water and has an ammonia-like odor. Formamide is also used as an RNA stabilizer in gel electrophoresis by deionizing RNA. In capillary electrophoresis, it is used for stabilizing (single) strands of denatured DNA. Formamide has also been put forward as an alternative solvent to water, perhaps with the ability to support life with alternative biochemistries to that found on earth [4]. The nitrosamines constitute a family of potent carcinogenic compounds, which are formed readily from various nitrogen compounds such as nitrite and their various derivatives [5,6]. In this work, characteristics of hydrogen bonds that exist in complexes between nitrosamine–formamide and nitrosamine–formic acid are completely investigated by a DFT approach.

2. Calculation methods

All the structures studied in this work were optimized by using B3LYP [7–9] with 6-311++G(2d,2p) [10,11], (aug-cc-pVDZ) [12,13] and (aug-cc-pVTZ) [14] basis sets. It has been demonstrated that B3LYP and MP2 levels of theory give similar results [15]. Vibrational frequency calculations were carried out for all complexes at the B3LYP/aug-cc-pVDZ and the B3LYP/aug-cc-pVDZ levels to calculate the zero point energy (ZPE). For the all complexes, the basis set superposition errors (BSSE) [16] were computed using the counterpoise method. In addition, fragment relaxation energy (E_{rel}) correction to counterpoise method was incorporated employing

* Corresponding author. Tel.: +98 9155436373.
  E-mail address: s.ali.bavafa@Gmail.com (S. Bavafa).

$E_{rel}(A) = E_{AB}(A) - E_A(A)$, with $E_{AB}(A)$ the energy of monomer A in dimer geometry. The NBO analysis was carried out by NBO program version 3.1 [17] included in Gaussian 03 [18] program at the B3LYP/aug-cc-pVDZ level. The Bader's Atoms in Molecules (AIM) theory [19,20] was also applied to find critical points and to characterize them. Topological properties were calculated at the B3LYP/aug-cc-pVDZ level of theory by the AIM2000 program package [21].

3. Results and discussion

During the computation, 15 complexes were found. Six structures belong to the interaction of nitrosamine with Z-rotamer of formic acid, four structures related to the E-rotamer of formic acid, and five other structures belong to formamide. All complexes were identified to be real minimum energy structures without any imaginary frequency. The optimized structures are shown in Figs. 1 and 2. Table 1 shows the results of computations at B3LYP level of theory and 6-311++(2d,2p), aug-cc-pVDZ and aug-cc-pVTZ basis sets.

The order of bond strength between nitrosamine and formic acid (Z- and E-rotamers) are as follows: Z-1(−10.08) > Z-2(−8.98) > E-1(−6.44) > E-2(−6.38) > E-3(−5.58) > Z-3(−5.13) > E-4(−5.10) > Z-4(−4.75) > Z-5(−2.06) > Z-6(−1.99). Also the order of bond strength between nitrosamine and formamide is: F-1(−9.34) > F-2(−8.75) > F-3(−6.55) > F-4(−6.35) > F-5(−3.49). Inside the parentheses is the energy (kcal/mol) of bond formation plus ΔZPE (D_0) at aug-cc-pVTZ. According to Table 1, the complexes of Z-1 and F-1 are the most stable ones for the all methods.

Bond formation energy corrected with ZPE and BSSE (D_0^{BSSE}) for Z-1 and F-1 complexes have −9.86 and −9.10 kcal/mol at B3LYP/aug-cc-pVTZ, −10.01 and −9.32 kcal/mol at B3LYP/aug-cc-pVDZ, −9.67 and −8.78 kcal/mol at B3LYP/6-311++(2d,2p).

Z-1 complex has two hydrogen bonds of O–H···O and N–H···O, and F-1 complex has two N–H···O. Order of hydrogen bond strength reduces as follows (see Section 3.2): O–H···O > N–H···O > N–H···N > C–H···O > C–H···N. This subject shows that the proton stretching between donor and acceptor affect the strength of hydrogen bond. Whenever acceptor and donor are homo-nuclear oxygen, the hydrogen bond is stronger than the case that acceptor and donor are homo-nuclear nitrogen.

It is clear that with increasing electronegativity of acceptors and donors, hydrogen bond becomes stronger. Bond length and angles of Z-NA and F-NA at B3LYP/aug-cc-pVTZ are shown in Table 2. Eight-member ring complexes of Z-1 and F-1 have resonance-assisted hydrogen bonds (RAHB) mechanism. Because the length of C1=O2 and N7=O8 in these complexes have been increased by 0.016, 0.019, 0.015 and 0.017, respectively. C1–O3 and C1–N11 in Z-1 and F-1 complexes has been reduced by 0.029 and 0.018, respectively. Z-2 and F-2 complexes have also RAHB mechanism. This means that the Π-electron delocalization causes a strengthening of the hydrogen bond [22,23]. However, effect of RAHB mechanism in these complexes are weaker than Z-1 and F-1; because, N=O is directed outside of the ring. In Z-2 and F-2 complexes, N=O is directed toward the ring, but relative to the complexes with directed outside of the ring have weaker RAHB mechanism. The reason is that O3–H5 plays a role of both acceptor and donor.
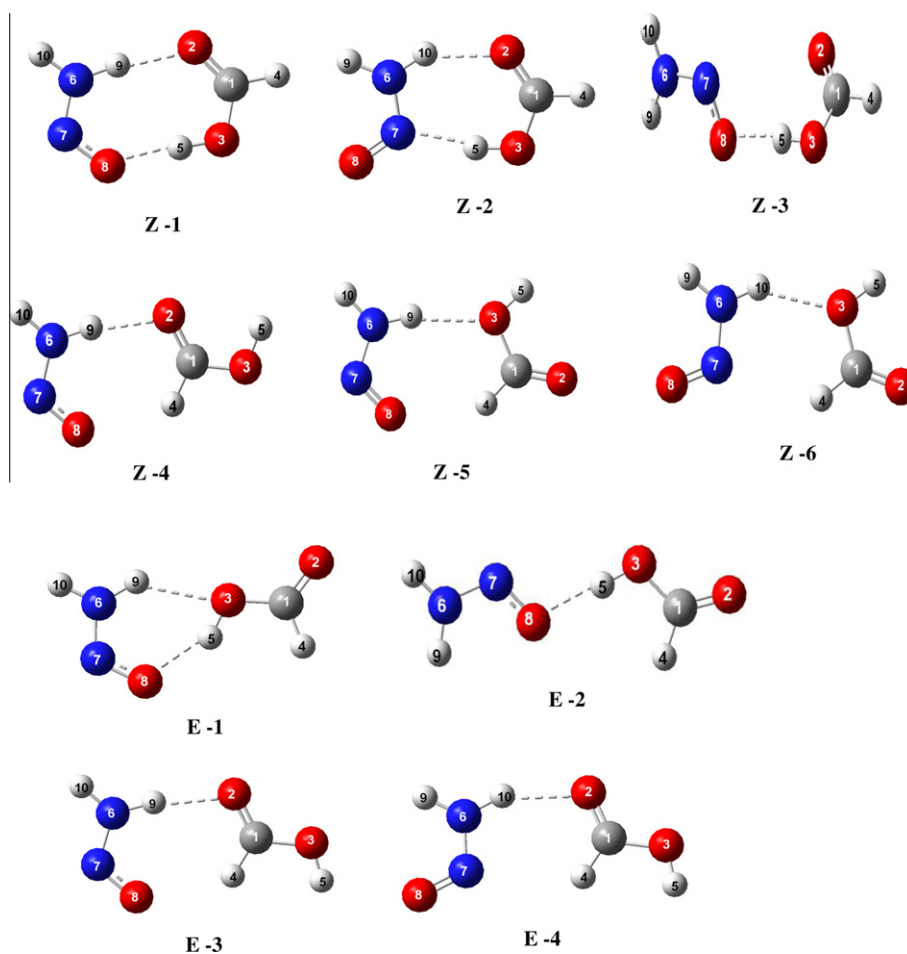

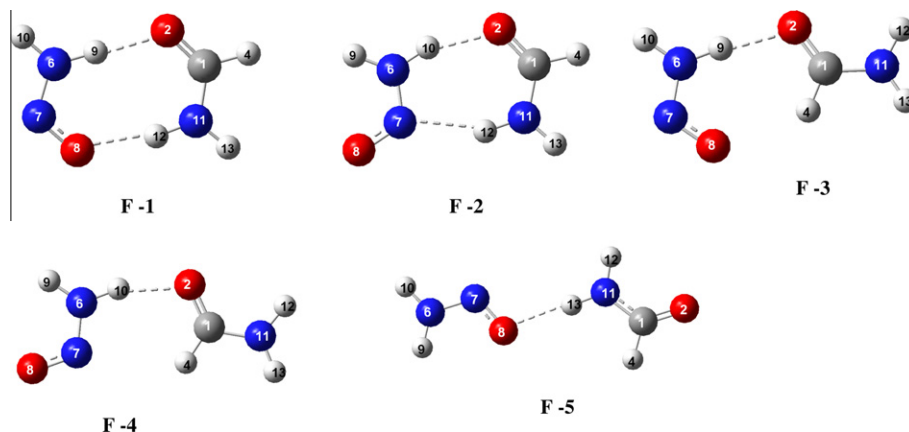**Fig. 1.** The complexes formed by formic acid (Z and E) and nitrosamine.

Fig. 2. The complexes formed by formamide and nitrosamine.

Table 1
Binding energies (kcal/mol) of nitrosamine–formic acid (Z and E), and nitrosamine–formamide (F) complexes. For the structures of complexes, see Fig. 1.

Complex	D_0^a	BSSE^a	D_0^{BSSEa}	D_0^b	BSSE^b	D_0^{BSSEb}	D_0^c	BSSE^c	D_0^{BSSEc}
Z-1	−10.06	0.39	−9.67	−10.61	0.60	−10.01	−10.08	0.22	−9.86
Z-2	−9.02	0.45	−8.57	−9.36	0.53	−8.83	−8.98	0.21	−8.77
Z-3	−5.21	0.28	−4.93	−5.33	0.30	−5.03	−5.13	0.13	−5.00
Z-4	−4.92	0.25	−4.68	−5.21	0.52	−4.69	−4.75	0.14	−4.60
Z-5	−2.24	0.14	−2.10	−2.37	0.32	−2.05	−2.06	0.13	−1.93
Z-6	−2.09	0.19	−1.90	−2.20	0.43	−1.77	−1.99	0.15	−1.84
E-1	−6.55	0.33	−6.22	−6.76	0.48	−6.28	−6.44	0.19	−6.25
E-2	−6.49	0.32	−6.17	−6.58	0.51	−6.07	−6.38	0.18	−6.2
E-3	−5.77	0.26	−5.51	−6.07	0.53	−5.54	−5.58	0.15	−5.43
E-4	−5.22	0.18	−5.04	−5.49	0.39	−5.10	−5.10	0.13	−4.97
F-1	−9.36	0.58	−8.78	−9.96	0.64	−9.32	−9.34	0.24	−9.10
F-2	−8.73	0.56	−8.17	−9.26	0.60	−8.66	−8.75	0.19	−8.56
F-3	−6.65	0.34	−6.31	−7.04	0.34	−6.70	−6.55	0.13	−6.42
F-4	−6.38	0.47	−5.91	−6.74	0.47	−6.27	−6.35	0.15	−6.20
F-5	−3.56	0.11	−3.44	−3.72	0.34	−3.38	−3.49	0.10	−3.39

$D_0 = D_e$ (electronic binding energy) + ΔZPE, $D_0^{BSSE} = D_0$ + BSSE.
[a] 6-311++G(2d,2p).
[b] aug-cc-pVDZ.
[c] aug-cc-pVTZ.

Table 2
Optimized geometrical parameters for monomers (Z, F, NA) and complexes at B3LYP/aug-cc-pVTZ level.

Parameter	Z^a	F^b	NA^c	Z-1^d	Z-2^d	Z-3^d	Z-4^d	Z-5^d	Z-6^d	F-1^d	F-2^d	F-3^d	F-4^d	F-5^d
C1=O2	1.198	1.211		1.214	1.212	1.203	1.207	1.196	1.195	1.226	1.224	1.223	1.221	1.215
C1–H4	1.096	1.104		1.096	1.095	1.098	1.094	1.094	1.095	1.100	1.100	1.099	1.010	1.104
C1–O3	1.345			1.316	1.321	1.332	1.335	1.360	1.359					
O3–H5	0.970			0.998	0.994	0.987	0.971	0.970	0.970					
C1–N11		1.357								1.339	1.342	1.347	1.347	1.351
N11–H12		1.007								1.020	1.018	1.007	1.007	1.007
N11–H13		1.004								1.004	1.004	1.004	1.004	1.011
N7=O8			1.213	1.232	1.216	1.223	1.222	1.218	1.215	1.230	1.220	1.224	1.220	1.219
N6–N7			1.325	1.301	1.309	1.309	1.316	1.320	1.320	1.306	1.309	1.313	1.313	1.314
N6–H9			1.015	1.032	1.014	1.016	1.025	1.018	1.015	1.034		1.032	1.016	1.016
N6–H10			1.005	1.006	1.018	1.006	1.005	1.005	1.008		1.024	1.005	1.020	1.005
O2(3)···H9(10)				1.849	1.937		1.966	2.171	2.178	1.832	1.854	1.856	1.881	
H4(5 or 12)···N7					1.876					2.781	2.143		2.907	
H4(5, 12 or 13)···O8				1.727		1.802	2.459	2.517		1.953		2.452		2.068
C1–H4···O8 or N7							130.163	141.460	130.090			132.610	117.430	
N6–H9(10)···O2(3)				172.620	148.930		170.779	167.430	148.250	179.500	160.530	174.260	162.440	
O3–H5···O8 or N7				176.610	169.010	175.352								
N11–H12(13)···O8										168.600				177.792
N11–H12···N7											154.370			

[a] Z-rotamer of formic acid.
[b] Formamide.
[c] Nitrosamine.
[d] Complexes shown in Fig. 1.

Hydrogen bond distances in homo-nuclear oxygen Z-1 and Z-3 complexes (H5···O8) are 1.727 and 1.803 Å, respectively. The hydrogen bond distance in heteronuclear nitrogen in F-1 complex (H9···O2) is 1.832 Å. According to the above results and Table 2, the minimum hydrogen bond distance belongs to homo-nuclear oxygen. There is a linear relationship between hydrogen bond angle and its distance. Probably, this may be caused by the directional electrostatic interactions such as dipole–dipole interactions between formic acid and formamide with NH_2NO. In the absence of experimental data, it is a hard task to distinguish between blue shift and red shift because contrasting results have been obtained by B3LYP and MP2 calculations [24]. Tables 3 and 4 show stretching frequencies, blue and red shifts in symmetric and asymmetric O–H, C–H and N–H mixed with O–H stretching in monomer and complexes at B3LYP/aug-cc-pVDZ. Bond lengths of O–H and N–H increase during bond formation. This shows red shifts in frequencies. Red shifts in stretching frequency of O–H are a common fingerprint at hydrogen bond. Stretching frequency of O–H in hydrogen bond is mixed with symmetric and asymmetric stretching frequency of N–H.

In Z-1 which has the strongest RAHB mechanism, stretching frequency of O–H is mixed with symmetric and asymmetric stretching frequency N–H. These have 3126 and 3207 values, respectively. The red shifts are −322 and −485, respectively. Tables 3 and 4 show that the complexes that have RAHB mechanism, O–H stretching frequency is mixed with stretching frequency of N–H. F-1 stable complex has two stretching frequencies of symmetric N–H and asymmetric stretching of NH_2 in nitrosamine and formamide. N–H from formamide contributes in N11–H12···N7 and N11–H12···O8 hydrogen bonds in F-1 and F-2 complexes. Asymmetric stretching frequency of N–H in N11–H12···O8 is equal to 3358 (−211) and in N11–H12···N7 is equal to 3399 (−170). It shows that proton accepting of oxygen is greater than proton accepting of nitrogen. Bond length of C1–H4 reduces, so blue shift occurs. For Z-4, Z-5, Z-6, F-3 and F-4 at B3LYP/aug-cc-pVDZ the shift values are 39, 31, 20, 56 and 71, respectively.

3.1. Natural bond orbital analyses

The formation of a hydrogen bond implies that a certain amount of electronic charge is transferred from the proton acceptor to the proton donor molecule [25,26]. Furthermore, there is a rearrangement of electron density within each monomer. By NBO analysis, Reed et al. [27] for several typical Hydrogen bond systems have demonstrated that the charge is transferred from the lone pairs of the proton acceptors to the antibonding orbitals of the proton donors. The results of NBO analyses including charge transfer energy, natural charge, and the occupancy of NBOs at B3LYP/aug-cc-pVDZ level of theory are given in Tables 5 and 6. The charge

transfer can be defined as the sum of the atomic charges on complexed NH_2NO. The NBO analyses show that the electronic charge is transferred from formic acid and formamide to NH_2NO in these complexes except for Z-5 and Z-6. Comparison of charges shows that the interacting hydrogen atoms of monomers lose electronic charge upon complex formation, as expected for conventional hydrogen bonding. This well-known effect constitutes another Koch–Popelier criterion [28] and is one of the main characteristics of the interaction.

The O atoms involved in the interaction gains electronic charge upon complex formation. The NBO results show that the specific $lp(N6) \rightarrow \sigma^*$ (N7=O8), $lp(O3) \rightarrow \sigma^*(C1=O2)$ and $lp(N11) \rightarrow \sigma^*(C1=O2)$ interactions are the most important interactions in NH_2NO, formic acids, and formamide, respectively. The energy value of these interactions increases upon complex formation. The charge transfer energy associated with $lp(N6) \rightarrow \sigma^*(N7=O8)$ interaction is 73.25 kcal/mol in NH_2NO which increases to 98.67, 88.92, 79.56, 83.42, 78.78 and 77.58 kcal/mol in complexes from Z-1 to Z-6, to 88.78, 86.11, 85.38 and 81.84 kcal/mol in complexes from E-1 to E-4 and to 94.19, 88.66, 85.84, 84 and 80.95 kcal/mol in complexes from F-1 to F-5, respectively. The greater charge transfer energy obtained for Z-1 and F-1 confirms their stronger RAHB mechanism. The interactions $lp(O \text{ or } N) \rightarrow \sigma^*((N–H) \text{ or } (C–H) \text{ or } (O–H))$ are the most important intermolecular interactions that have key role in stability of complexes. The greater charge transfer energy is in consistent with the greater population of acceptor orbital (σ^*). The population of $\sigma^*(O3–H5)$ (0.0778 a.u.) in Z-1 is greater than other complexes.

3.2. Atoms in molecules (AIM)

Bader's theory of atoms in molecules (AIM) [19] is one of the widely used theoretical tools to understand the hydrogen bond interaction. Popelier and coworkers have employed the AIM theory to address several important chemical issues [29,30]. Critical points (CPs) of the electron density are points where the gradient of $\rho(r)$ vanishes. According to the AIM theory, the essential condition to detect an A–H···B hydrogen bond is the existence of a $(3, -1)$ bond critical point (BCP) at the H···B path and some of its properties have been proposed to set the criteria to characterize hydrogen bond [31,32]. The values of electron density, $\rho(r)$, its corresponding Laplacian, $\nabla^2 \rho(r)$, electronic energy density, $H(r)$ (electronic kinetic energy density $G(r)$ + electronic potential energy density, $V(r)$) at the BCPs were calculated at B3LYP/aug-cc-pVDZ level of theory are listed as electronic supporting information. Table 7 shows topological properties of the bond critical points of the intermolecular hydrogen bonds.

Since it was pointed out that some of the intermolecular homo-nuclear RAHBs may be treated as partly covalent in nature, the

Table 3
Harmonic frequencies (in cm^{-1}) and shifts (red and blue) for some selected vibrational modes at B3LYP/aug-cc-pVDZ.

	O–H stretching mode[d]		N–H symmetric stretching mode[c]		N–H asymmetric stretching mode[c]		C–H stretching mode[d]	
	Freq	Shift	Freq	Shift	Freq	Shift	Freq	Shift
Z	3717	–	–	–	–	–	3065	
NA	–	–	3448	–	3692	–	–	–
Z-1	–	–	3126[a]	−322	3207[b]	−485	–	–
Z-2	3225	−492	3360	−88	3563	−129	–	–
Z-3	3384	−333	–	–	–	–	–	–
Z-4	–	–	3294	−154	3666	−26	3104	39
Z-5	–	–	3409	−39	3679	−13	3096	31
Z-6	–	–	3439	−9	3642	−50	3085	20

[a] The mixing modes of O–H and NH_2 symmetric.
[b] The mixing modes of O–H and NH_2 asymmetric.
[c] In nitrosamine.
[d] In formic acid.

Table 4
Harmonic frequencies (in cm^{-1}) and shifts (red and blue) for some selected vibrational modes at B3LYP/aug-cc-pVDZ.

	N–H symmetric stretching mode[a]		N–H asymmetric stretching mode[a]		N–H symmetric stretching mode[b]		N–H asymmetric stretching mode[b]		C–H stretching mode	
	Freq	Shift	Freq	Shift	Freq	Shift	Freq	Shift	Freq	Shift
F	3569	–	3715	–	3448	–	3692	–	2958	–
F-1	3358	−211	3672	−43	3110	−338	3647	−45	2999	–
F-2	3399	−170	3672	−43	3258	−189	3529	−163	3004	–
F-3	3567	–	3712	–	3311	−137	3530	−162	3014	56
F-4	3567	–	3712	–	3168	−280	3655	−37	3029	71
F-5	3494	−75	3664	−51	–	–	–	–	–	

[a] In formamide.
[b] In nitrosamine.

Table 5
Natural Bond Orbital (NBO) analyses of intermolecular hydrogen bonds at B3LYP/aug-cc-pVDZ.

Atoms	Z	NA	Z-1	Z-2	Z-3	Z-4	Z-5	Z-6
C1[a]	0.6934		0.7176	0.7143	0.6951	0.7015	0.6840	0.6864
O2[a]	−0.6103		−0.6742	−0.6704	−0.6330	−0.6518	−0.6023	−0.5978
O3[a]	−0.7223		−0.7224	−0.7254	−0.7436	−0.7071	−0.7560	−0.7559
H4[a]	0.1357		0.1399	0.1413	0.1214	0.1701	0.1659	0.1564
H5[a]	0.5035		0.5173	0.5072	0.5186	0.5050	0.5105	0.5117
N6[a]		−0.6211	−0.5807	−0.5896	−0.5830	−0.6090	−0.6126	−0.6157
N7[a]		0.2155	0.2307	0.1678	0.2419	0.2129	0.2177	0.2019
O8[a]		−0.3965	−0.4665	−0.3907	−0.4361	−0.4410	−0.4228	−0.4025
H9[a]		0.3911	0.4279	0.3969	0.4010	0.4176	0.4094	0.3916
H10[a]		0.4110	0.4104	0.4486	0.4176	0.4020	0.4061	0.4240
E(2) (kcal/mol)								
LPO2 (3) → σ*N6–H9 (10)			21.06	13.65		13.01		
LPO8 → σ*C1–H4						2.23	2.31	
LPN6 → σ*N7=O8		73.25	98.67	88.92	79.56	83.42	78.78	77.58
LPO3 (or N11) → σ*C1=O2	55.28		71.09	68.38	61.94	58.98	48.83	49.26
LPN7(or O8 or O2) → σ*C1–H4 (or N11)						19.74	2.31	1.41
LPO8 (or N7) → σ*O3–H5			29.05	20.15	34.13			
LPO2→σ*C1=O3					32.81	31.67		
σC1–H4[b]	0.0648					0.0623	0.0646	0.0654
σN6–H9[b]		0.0358	0.0699				0.0437	
σ*N6–H10[b]		0.0119		0.0383			0.0563	0.0207
σO3–H5[b]	0.0156		0.0778	0.0777	0.0537			

[a] Charges calculated by NBO.
[b] Occupation calculated by NBO.

Table 6
Natural Bond Orbital (NBO) analysis of intermolecular hydrogen bonds (NH$_2$NO with formamide) at B3LYP/aug-cc-pVDZ.

Atoms	F	NH$_2$NO	F-1	F-2	F-3	F-4	F-5
C1[a]	0.5540		0.5630	0.5628	0.5512	0.5542	0.5521
O2[a]	−0.6345		−0.6858	−0.6807	−0.6741	−0.6691	−0.6539
H4[a]	0.1255		0.1411	0.1429	0.1686	0.1541	0.1237
N11[a]	−0.8748		−0.8613	−0.8623	−0.8557	−0.8548	−0.8817
H12[a]	0.4185		0.4429	0.4316	0.4203	0.4224	0.4094
H13[a]	0.4112		0.4136	0.4156	0.4197	0.4204	0.4277
N6[a]		−0.6211	−0.5920	−0.6007	−0.6087	−0.6134	−0.5940
N7[a]		0.2155	0.2144	0.1713	0.2015	0.1914	0.2266
O8[a]		−0.3965	−0.4684	−0.4152	−0.4482	−0.4271	−0.4257
H9[a]		0.3911	0.4259	0.3882	0.4224	0.3818	0.4003
H10[a]		0.4110	0.4067	0.4464	0.4029	0.4401	0.4156
E(2) (kcal/mol)							
LPO2 (3) → σ*N6–H9 (10)			22.70	19.27	19.23	16.27	
LPO8 (2) → σ*C1–H4 (or N11)					2.34		
LPN6 → σ*N7=O8		73.25	94.19	88.66	85.84	84	80.95
LPO8 (or N7) → σ*N11–H12(13)			14.21	8.77			25.5
LPN11 → σ*C1=O2	62.86		76.32	74.81	67.66	67.86	67.19
σ*C1–H4[b]	0.0702				0.0641	0.0623	
σ*N6–H9[b]		0.0358	0.0747		0.0676		
σ*N6-H10[b]		0.0119		0.0499		0.0430	
σ*N11–H12(13)[b]	0.0143		0.0464	0.0436			0.0276

[a] Charges calculated by NBO.
[b] Occupation calculated by NBO.

Table 7
Topological properties of the bond critical points of the intermolecular hydrogen bonds.

Bond	$\rho(r)$	$\nabla^2 \rho(r)$	$H(r)$	$\rho(r)$	$\nabla^2 \rho(r)$	$H(r)$	$\rho(r)$	$\nabla^2 \rho(r)$	$H(r)$
	NH$_2$NO				F				
N6–H9	0.3277	−1.5081	−0.4216						
N6–H10	0.3378	−1.5871	−0.4411						
C1–H4				0.2749	−1.0215	−0.2881			
N11–H12				0.3350	−1.5535	−0.4348			
							Z		
O3–H5							0.3509	−2.0567	−0.5781
C1–H4							0.2820	−1.1093	−0.3057
	Z-1			Z-2			Z-3		
O3–H5	0.3157	−1.8273	−0.5190	0.3209	−1.8412	−0.5237	0.3290	−1.9445	−0.5485
N6–H9(10)	0.3109	−1.4577	−0.4052	0.3229	−1.5509	−0.4282			
O8(or N7)...H5	0.0421	0.1339	0.0004	0.0366	0.1005	0.0009	0.0346	0.1173	0.0250
O2...H9(10)	0.0337	0.1087	0.0014	0.0283	0.0909	0.0012			
	Z-4			Z-5			Z-6		
N6–H9(10)	0.3179	−1.4821	−0.4124	0.3248	−1.5100	−0.4202	0.3339	−1.5854	−0.4388
O8(N7)...H4	0.0107	0.0310	0.0072	0.0094	0.0269	0.0003	0.0067	0.0189	0.0005
O2(3)...H9(10)	0.0256	0.0790	0.0174	0.0154	0.0470	0.0007	0.0152	0.0484	0.0007
	F-1			F-2			F-3		
C1–H4									
N6–H9(10)	0.3076	−1.4331	−0.3992	0.3170	−1.5131	−0.4192	0.3105	−1.4425	−0.4022
O2...H9(10)	0.0353	0.1116	0.0011	0.0336	0.1085	0.0013	0.0330	0.1040	0.0012
N11–H12	0.3212	−1.5142	−0.4211	0.3240	−1.5185	−0.4229			
O8...H4(12)	0.0267	0.0813	0.0010				0.0113	0.0311	0.0001
N7(11) (or C1)–H12(4)				0.0213	0.0566	0.0008	0.2811	−1.1062	−0.3049
	F-4			F-5					
O2(8)...H10(13)	0.0309	0.1004	0.0015	0.0204	0.0617	0.0007			
N6(11)–H10(13)	0.3213	−1.5317	−0.4243	0.3303	−1.5404	−0.4309			
C1–H4	0.2795	−1.0788	−0.2995						
H4...N7	0.0052	0.0165	0.0006						

decomposition of the interaction energy for these intermolecular RAHBs provides a powerful tool to better understand the nature of such connections and to investigate what does the term "covalent" exactly mean. If values of ρ_c at the two bond paths of A–H···O indicate that the electron redistribution decreases $\rho(r)$ in the covalent bond A–H and increases it in the hydrogen bond H···O as A···O intermolecular distance shortens, the Laplacian of $\rho(r)$ tells how this redistribution affects the bond environment locally. Let us recall that in the AIM theory, strong shared-shell interatomic interactions (such as a covalent bond) are characterized by local concentration of charge ($\nabla^2 \rho(r) < 0$) and thus the BCPs of covalent bonds have negative $\nabla^2 \rho(r)$, whereas weak closed-shell interactions (such as a hydrogen bond) exhibit local depletion of

charge ($\nabla^2 \rho(r) > 0$) and the BCPs of hydrogen bonds have positive $\nabla^2 \rho(r)$ [28]. According to other Koch–Popelier criteria, these values must be in the range $\nabla^2 \rho(r) = 0.02$–0.15 a.u. [28].

The local value of the total energy density at a point r, $H(r)$, is another useful topological descriptor that provides supplementary information about the nature of the interaction at r. The total energy density $H(r)$ is the sum of the kinetic energy density $G(r)$, a positive quantity, and the potential energy density $V(r)$, a negative quantity, both related to the Laplacian of $\rho(r)$ through the local expression for the virial theorem. For bonds with any degree or covalent character, $H(r)$ is than less zero, whereas for electrostatic interactions $H(r)$ is always greater than zero. The positive values of $\nabla^2 \rho(r)$ and $H(r)$ for the hydrogen bonds in this study indicate electrostatic interactions.

The comparison between $\rho(r)$ of the O–H···O, N–H···O and C–H···O hydrogen bonds shows that the homo-nuclear O–H···O hydrogen bond is stronger than heteronuclear N–H···O and C–H···O. The electron density in N6–H9 (10) and O3–H5 that contribute in hydrogen bond is reduced, by which, bond length of N6–H9 (10) and O3–H5 increases. This shows a red shift. However, electron density of C1–H4 in hydrogen bond increases and the bond length is reduced. The strongest HB, O–H···O, has the largest densities, $\rho = (0.0363$–0.0421 a.u.$)$, and the weak HBs, C–H···O have the smallest densities, $\rho = (0.0052$–0.0124 a.u.$)$. As shown in Fig. 3, there is a linear relationship between the electron density, $\rho(r)$ (a.u.), its corresponding Laplacian, $\nabla^2 \rho(r)$ (a.u.) and the bond distance O···H (Å) at B3LYP/aug-cc-pVDZ level of theory.

$$\rho(r) = 2.66\text{-}24.9\, d_{\text{O···H}}$$
$$R^2 = 0.934$$

$$\nabla^2\rho(r) = 2.61\text{-}7.31\, d_{\text{O···H}}$$
$$R^2 = 0.931$$
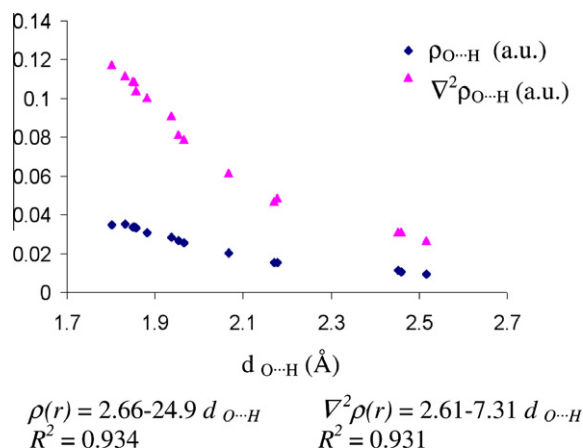
Fig. 3. Correlation between the electron density, $\rho(r)$ (a.u.), its corresponding Laplacian, $\nabla^2 \rho(r)$ (a.u.) and the bond distance O···H (Å) at B3LYP/aug-cc-pVDZ level of theory.

4. Conclusion

During the computation, 15 stable complexes were found. Six structures belong to the interaction of nitrosamine with formic acid (Z), four structures related to the formic acid (E), and five other

structures belong to formamide. In all methods B3LYP/6-311++(2d,2p), B3LYP/aug-cc-pVDZ and B3LYP/aug-cc-pVTZ, the complexes of Z-1 and F-1 are the most stable ones. The Z-rotamer complex is more stable in the gas phase. The NBO results show that the specific $lp(N6) \rightarrow \sigma^*(N7=O8)$, $lp(O3) \rightarrow \sigma^*(C1=O2)$ and $lp(N11) \rightarrow \sigma^*(C1=O2)$ interactions are the most important interactions in NH_2NO, formic acids and formamide respectively. From AIM data, it can be concluded that the homo-nuclear O–H$\cdots$O, H-bond in complexes is stronger than heteronuclear N–H$\cdots$O and C–H$\cdots$O.

References

[1] S.Y. Liu, D.M. Mehringer, L.E. Snyder, J. Astrophys. 552 (2001) 654.
[2] A. Goldman, F.H. Murcray, D.G. Murcray, C.P. Rinsland, Geophys. Res. Lett. 11 (1984) 307.
[3] M.S. Ermelinda, J. Lundell, M. Pettersson, L. Khriachtchev, R. Fausto, M. Räsänen, J. Mol. Spectrosc. 219 (2003) 70.
[4] http://www.astrobio.net/news/article2171.html.
[5] F. Murad, Angew. Chem. Int. Ed. 38 (1999) 1856.
[6] P. Jiang, Q. Ximei, L. Chunhui, Q. Chunhui, W. Dianxun, Chem. Phys. Lett. 508 (1997) 277.
[7] C. Lee, W. Yang, R.G. Parr, Phys. Rev. B 37 (1988) 785.
[8] A.D. Becke, J. Chem. Phys. 98 (1993) 1372.
[9] P.J. Stephens, F.J. Devlin, C.F. Chabalowski, M.J. Frisch, J. Phys. Chem. 98 (1994) 11623.
[10] R. Krishnan, J.S. Binkley, R. Seeger, J.A. Pople, J. Chem. Phys. 72 (1980) 650.
[11] J.P. Blaudeau, M.P. McGrath, L.A. Curtiss, L. Radom, J. Chem. Phys. 107 (1997) 5016.
[12] T.H. Dunning, J. Chem. Phys. 90 (1989) 1007.
[13] D.E. Woon, T.H. Dunning, J. Chem. Phys. 98 (1993) 1358.
[14] R.A. Kendall, T.H. Dunning, R.J. Harrison, J. Chem. Phys. 96 (1992) 6796.
[15] (a) A. Hocquet, N. Leulliot, M. Ghomi, J. Phys. Chem. B 104 (2000) 10934;
(b) M.P. Gaigeot, N. Leulliot, M. Ghomi, H. Jobic, O. Bouloussa, C. Coulombeau, Chem. Phys. 217 (2000) 261;
(c) S. Simon, M. Sodupe, J. Bertain, J. Phys. Chem. A 106 (2002) 5397;
(d) J. Bertain, L. Rodriguez-Santiago, M. Bodupe, J. Phys. Chem. B 103 (1999) 2310.
[16] S.F. Boys, F. Bernardi, Mol. Phys. 19 (1990) 553.
[17] E.D. Glendening, A.E. Reed, J.E. Carpenter, F. Weinhold, NBO, Version 3.1
[18] M.J. Frisch et al., Gaussian 03, Revision B03, Gaussian Inc., Pittsburgh PA, 2003.
[19] R.F.W. Bader, Atoms in Molecules. A Quantum Theory, Clarendon Press, Oxford, 1990.
[20] R.F.W. Bader, H. Essen, J. Chem. Phys. 80 (1994) 1943.
[21] F. Biegler-König, J. Schönbohm, D. Bayles, J. Comp. Chem. 22 (2001) 545.
[22] G. Gilli, F. Belluci, V. Ferretti, V. Bertolasi, J. Am. Chem. Soc. 111 (1989) 1023.
[23] V. Bertolasi, P. Gilli, V. Ferretti, G. Gilli, J. Am. Chem. Soc. 113 (1991) 4917.
[24] P. Lu, G.-Q. Liu, J.-C. Li, J. Mol. Struct. (THEOCHEM) 723 (2005) 95.
[25] P. Hobza, Z. Havlas, Chem. Rev. 4253 (2000) 4253.
[26] P. Hobza, V. Spirko, H.L. Selzle, E.W. Schlag, J. Phys. Chem. A 102 (1998) 2501.
[27] A.E. Reed, L.A. Curtiss, F. Weinhold, Chem. Rev. 88 (1988) 899.
[28] U. Koch, P.L.A. Popelier, J. Chem. Phys. 99 (1995) 9747.
[29] P.L.A. Popelier, Atoms in Molecules. An Introduction, Prentice-Hall, Harlow, UK, 2000.
[30] P.L.A. Popelier, Coord. Chem. Rev. 197 (2000) 169.
[31] S.J. Grabowski, J. Phys. Org. Chem. 17 (2004) 18.
[32] P.L.A. Popelier, P.J. Smith, Quantum topological atoms, in: A. Hinchliffe (Ed.), Chemical Modelling Applications and Theory, vol. 2, The Royal Society of Chemistry, London, 2002, p. 391 (Chapter 8).